

Axial flow hydraulic pulse testing of an argillaceous limestone

A. P. S. Selvadurai · A. Letendre · B. Hekimi

Received: 11 May 2010 / Accepted: 11 March 2011 / Published online: 29 March 2011
© Springer-Verlag 2011

Abstract Lindsay Limestone is an argillaceous limestone encountered in Southern Ontario, Canada. The Lindsay formation is regarded as a suitable geologic medium for the construction of a Deep Geologic Repository for storing low to intermediate level nuclear waste. The Lindsay Limestone is a nodular argillaceous rock with very low permeability, requiring the use of hydraulic pulse tests for the measurement of its permeability characteristics. The paper describes the triaxial testing facility, the theoretical basis for the test and the procedures used to analyze the experimental results for estimating the permeability of the Lindsay Limestone. The results are compared with the data available in the literature.

Keywords Axial flow pulse tests · Permeability measurement · Lindsay Limestone · Experimental modelling

Introduction

The development of methodologies for the storage of nuclear fuel waste has received concerted attention over the past half a century. In recent years, the topic has come to the forefront as a result of the climate change debate, where nuclear energy is viewed as an alternative to other forms of fossil fuel-based energy production, which emit significant amounts of greenhouse gases. The need for developing Deep Geologic Repositories for the safe storage of hazardous

spent nuclear fuel has been underscored by the recent (11 March 2011) earthquake and the resulting tsunami that inflicted damage to the nuclear reactor facilities at Fukushima, Japan. Comprehensive reviews of the storage concepts are given by Laughton et al. (1986), Chapman and McKinley (1987), OECD (1988), Gray (1993), Gnirk (1993) and Huertas et al. (2000). The general consensus points to the deep geological disposal of radioactive wastes in competent rocks that are considered to be stable in the time scales relevant to the storage of the wastes. Although the overall nuclear waste disposal concept relies on engineered barriers that also include the waste containers and engineered clay barriers (Pusch 1990; Hueckel et al. 1996; Selvadurai and Nguyen, 1996; Selvadurai 1997, 2002a; Hoteit et al. 2002; Alonso et al. 2002, 2005), it places a great deal of reliance on the geologic formation itself to act as a natural geological barrier to attenuate long-term radionuclide migration from the waste repository. The permeability of the geological formation that includes both intact and fractured regions is of central importance to the feasibility of the storage concept. The types of geological formations that have been targeted for high level nuclear waste disposal have included crystalline rock, similar to the granitic rocks found in countries, such as Canada, Finland, Japan, Sweden, and Switzerland; porous tuffs in the Western USA; dense clay and clay stone deposits in Europe, particularly Belgium, France, Spain and Switzerland. Recently, attention has focused on the possible use of clays and other sedimentary formations as host geologic media for siting deep ground repositories for the storage of nuclear wastes. An example is argillite at the Tournemire site in France that is being investigated for deep geological disposal of heat emitting nuclear fuel wastes (Armand and Su 2006; Millard and Rejeb 2008; Maßmann et al. 2009). The rationale for considering sedimentary formations is based on the specific

A. P. S. Selvadurai (✉) · A. Letendre · B. Hekimi
Department of Civil Engineering and Applied Mechanics,
McGill University, 817 Sherbrooke Street West,
Montreal, QC H3A 2K6, Canada
e-mail: patrick.selvadurai@mcgill.ca

geological attributes of a particular formation in terms of the assessments of historical groundwater movement patterns and on the beneficial aspects of sedimentary rocks, which are capable of mitigating the detrimental effects of underground excavations that can lead to damage zones and alterations in permeability. An example of a candidate sedimentary rock is the Lindsay formation in Southern Ontario, which is identified as a potential host rock for siting a repository for storing low and intermediate level nuclear wastes.

Proposals have been put forward for the construction of a deep geologic repository (DGR) would be constructed in the Paleozoic formation in the vicinity of the Bruce Nuclear Power Generating Station located on the shores of Lake Huron. The formation consists of a layered sequence of carbonates, shales, evaporites and minor sandstones. The sedimentary sequence is approximately 800-m thick and rests on the Precambrian basement. Extensive studies have been conducted to determine the stratigraphy, age, thickness and nomenclature of the sedimentary formations beneath the site of the Bruce Nuclear Power Generating Station. The suitability of the Middle Ordovician limestone sequences encountered at the Bruce site, and in particular the Lindsay formation, for the proposed siting of the DGR is discussed in the reports by Mazurek (2004), Vilks and Miller (2007) and OPG (2008). Argillaceous limestones in particular are known to possess self-healing properties (Horseman 2001), which are desirable attributes, particularly for nuclear waste management endeavours.

At the proposed location for the DGR, the geologic formations are nearly horizontally stratified and the approximately 45-m thick Middle Ordovician Lindsay formation is located almost 630 m below ground level. This sequence is overlain by Upper Ordovician Siltstone and Gray Shale (approximately 200-m thick) and underlain by Shaly Argillaceous limestone and Cambrian Sandstone sequences (approximately 150-m thick). The entire sequence of Paleozoic rocks rests on the Pre-Cambrian Granitic Gneiss (Fig. 1). The stratigraphic sequence was determined from both shallow boreholes and deep off-site gas exploration wells. The reports by Golder (2003), Mazurek (2004) and OPG (2008) also document the hydrogeological and geo-mechanical properties of the geologic strata encountered at the proposed DGR site. Of particular interest are the estimates for the hydraulic conductivity distribution with depth over the entire sequence of rocks, which ranges from 10^{-5} m/s in the upper dolostone to between 10^{-11} and 10^{-13} m/s in the Shaly limestone encountered immediately above the Precambrian Basement (Fig. 2). This translates to a permeability in the range 10^{-18} to 10^{-20} m² for a dynamic fluid viscosity of 10^{-6} kN s/m² and a fluid unit weight of approximately 10 kN/m³ (Table 1).

The main geologic horizon of interest to a DGR is the upper 45-m thick stratum of the Lindsay formation which

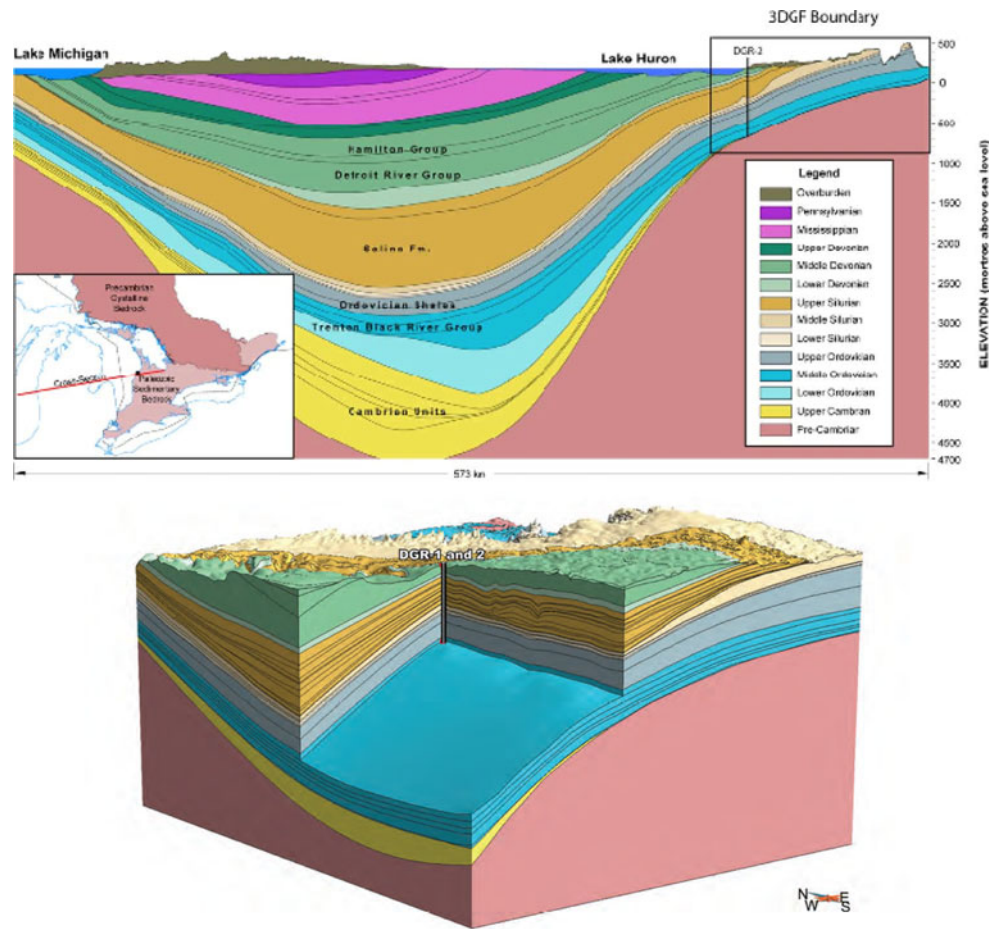
consists of fine-grained thin to medium bedded nodular textured argillaceous limestone. This sequence has the lowest hydraulic conductivity, and along with other attributes is considered to be a suitable formation for siting a DGR. The composition of the Lindsay Limestone is quite distinct from other limestones that are highly porous due to their vuggy nature that can result from cracks, fissures and stress-induced damage zones (Selvadurai 2004). This paper deals with the experimental determination of the permeability characteristics of the Lindsay Limestone using results of axial flow hydraulic pulse tests conducted on cylindrical samples with a diameter 100 mm. It describes the experimental procedures, the analytical details and the results of tests that lead to the estimation of the permeability characteristics of this low permeability rock.

Axial flow hydraulic pulse tests

Permeability of rocks and other geomaterials can be measured using either steady state tests or transient tests. The former is more suited for geomaterials with permeabilities up to 10^{-16} m², where steady state conditions can be established relatively conveniently and quickly (Selvadurai and Głowacki 2008; Selvadurai and Selvadurai 2007, 2010). For low permeability geomaterials with permeabilities $<10^{-19}$ m², steady state techniques are ineffective since the time required to establish a steady state condition is prohibitively long; the accurate interpretation of attainment of a steady state condition is difficult, because of the inability to conduct a fluid mass balance calculation accurately, making the steady state tests less reliable. The main advantage of the steady state test, however, is that there are virtually no extraneous parameters needed to interpret the results. Once the dimensions of the sample, the hydraulic gradient, the flow rate and the dynamic viscosity of the fluid at the test temperature are known, the permeability can be directly estimated.

Hydraulic pulse tests are transient tests that can be conducted relatively quickly to determine the permeability characteristics of low permeability geomaterials and are generally used for geomaterials with permeabilities $<10^{-19}$ m². The test involves the application of a fluid pressure pulse within a confined region in sealed contact with the open surface of a saturated geomaterial. The rate of pressure decay in the confined region depends, among other factors, on the permeability characteristics of the geomaterial. The main advantage of the hydraulic pulse test is the rapidity with which the test can be conducted. The disadvantage of the procedure is that a number of extraneous parameters are needed to conduct an analysis of the test, including the compressibility of the fluid used in the test, the compressibility of the pore skeleton and its porosity, the volume of fluid that is undergoing

Fig. 1 Regional Geological Framework and the Location of the DGR beneath the Bruce Site (OPG 2008)



(Approx. 40 x vertical exaggeration).

Table 1 Summary of reported permeability data on the Lindsay Limestone

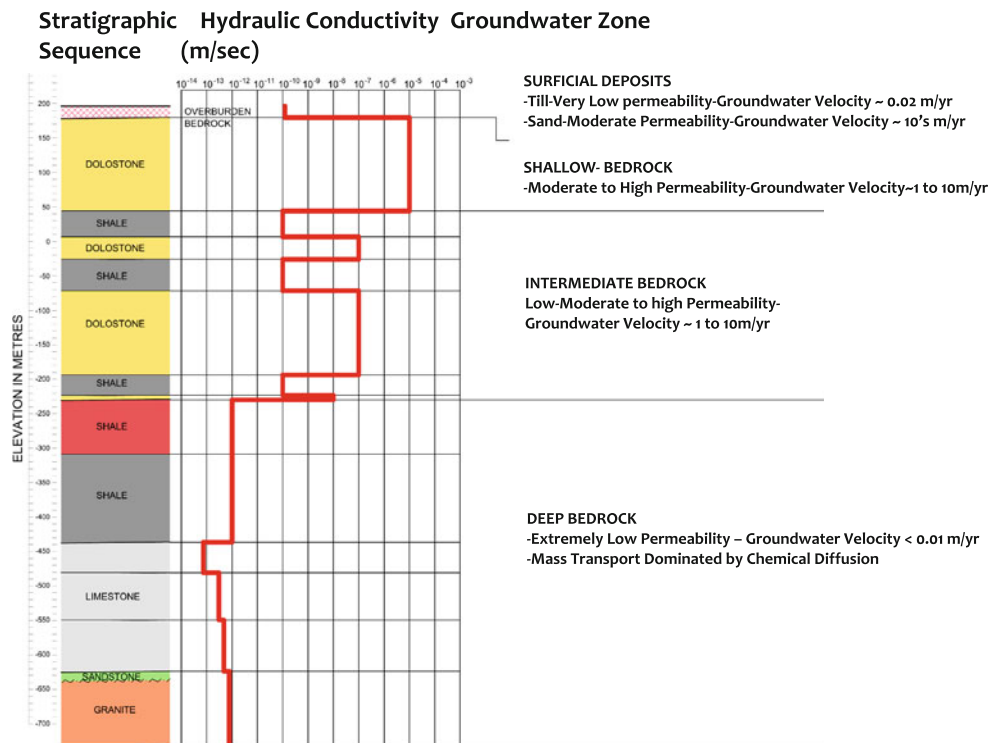
References	Location	K_{min} (m ²)	K_{max} (m ²)	K_{median} (m ²)
Raven et al. (1992)	OHD-1, Mississauga/Lakeview	1.02×10^{-20}	6.42×10^{-19}	3.26×10^{-19}
Raven et al. (1992)	UN-2, Darlington/Bowmanville	6.42×10^{-21}	1.63×10^{-18}	8.19×10^{-19}
Golder Associates (2003)	DDH01/02, Bowmanville	1.33×10^{-19}	4.08×10^{-18}	2.11×10^{-18}
Intera Ltd (1988)	Darlington generating station tunnels	1.02×10^{-18}	1.02×10^{-15}	5.11×10^{-16}
Intera Ltd (1988)	Wesleyville shallow boreholes	2.04×10^{-17}	4.08×10^{-13}	2.04×10^{-13}
Vilks and Miller (2007)	Cobourg perpendicular to bedding planes	$<10^{-22}$	3.50×10^{-22}	N/A
Vilks and Miller (2007)	Cobourg parallel to bedding planes	1.20×10^{-22}	2.20×10^{-21}	N/A
Gartner Lee Ltd (2008)	Cobourg vertical	N/A	N/A	9.79×10^{-20}
Gartner Lee Ltd (2008)	Cobourg horizontal	N/A	N/A	9.79×10^{-19}
Mazurek (2004)	In situ Packer tests in vertical or inclined boreholes	6.42×10^{-21}	4.08×10^{-18}	N/A

decompression and the ability to solve the transient initial boundary value problem of the pressure diffusion in a manner convenient for estimation of the permeability.

This research uses transient one-dimensional pulse tests to determine the permeability of the argillaceous Lindsay Limestone. The one-dimensional hydraulic pulse testing of

the permeability characteristics of rocks was pioneered by Brace et al. (1968) who determined the permeability of Westerly Granite under high confining pressures. The work of Hsieh et al. (1981), Neuzil et al. (1981) and Bernabé (1986, 1987) discuss the application of the technique for measuring the permeability characteristics of rocks,

Fig. 2 Variation of hydraulic conductivity at the DGR site. WWMF-LLW Geotechnical Feasibility Study (Golder Associates 2003)



including Chelmsford Granite and Barre Granite. Reviews of other applications of the hydraulic pulse tests for permeability testing are given by Selvadurai and Carnaffan (1997) and Gross and Scherer (2003) (measurement of permeability of cementitious materials) and Selvadurai et al. (2005) (measurement of permeability of granite cylinders, measuring 405 mm in diameter) and Song and Renner (2006) (permeability of Fontainebleau Sandstone). Recently, Selvadurai (2009) has examined the influence of residual hydraulic potentials and the degree of saturation on the performance of the axial flow pulse test. It was observed that low permeability can lead to residual hydraulic gradients introduced during saturation that can influence the transient response of a subsequent pulse test.

The theoretical concepts associated with hydraulic pulse tests are documented in many of the references cited previously and a brief summary is presented for completeness. We restrict attention to one-dimensional pressure transient phenomena in the saturated rock. The partial differential equation governing the transient pressure in an one-dimensional configuration is given by (see e.g. Bear 1972; Hsieh et al. 1981; Barenblatt et al. 1990; Philips 1991; Selvadurai 2000, 2002).

$$\frac{\partial^2 p}{\partial x^2} = \frac{S_s \eta}{K \gamma_w} \frac{\partial p}{\partial t}; \quad x \in (0, L_0) \quad (1)$$

where $p(x, t)$ is the fluid pressure (e.g. dimensions: M/LT^2), L_0 is the extent of the domain, η is the dynamic viscosity (dimensions: M/LT ; M refers to the dimension of mass

and T is the dimension of time), K is the permeability (dimensions: L^2), γ_w is the unit weight of water (dimensions: M/L^2T^2), S_s is the specific storage of the porous medium (dimensions: $1/L$), composed of a solid material that is non-deformable and defined by.

$$S_s = \gamma_w (nC_w + C_{\text{eff}}) \quad (2)$$

In (2), n is the porosity and C_w and C_{eff} (dimensions: LT^2/M) are, respectively, the compressibilities of the pore fluid and the porous skeleton. The solution of (1) is subject to the boundary conditions.

$$\Phi \left(\frac{\partial p}{\partial x} \right)_{x=0} = \left(\frac{\partial p}{\partial t} \right)_{x=0}; \quad p(L, t) = 0 \quad (3)$$

where

$$\Phi = \left(\frac{AK}{\eta V_w C_w} \right) \quad (4)$$

with V_w being the volume of fluid contained within the sample and the measurement unit and A is the cross-sectional area of the sample in contact with the pressurized region. The initial condition

$$p(x, 0) = 0; \quad x \in (0, L_0) \quad (5)$$

indicates that the tested region is initially under zero hydraulic head, which is necessary for the rigorous application of the simplified theoretical developments. The first boundary condition in (3) is a kinematic constraint indicating that the rate at which water flows from the cavity

into the sample, as expressed by Darcy’s law applied to the end of the sample, is equal to the rate at which the water stored within the pressurized region expands as the pressure within the system declines. The initial boundary value problem defined by Eqs. 1–5 is well posed, and has similarities to the analogous heat conduction problem. In particular, attention is focused on pressure transients in a semi-infinite domain, which makes the developments much simpler and replaces the boundary condition given by the second equation of (3) by a regularity condition requiring that $p(x, t) \rightarrow 0$ as $x \rightarrow \infty$ for $\forall t \geq 0$. If the pulse test is conducted by applying a hydraulic pulse in the form of a Dirac delta function of time then

$$p(0, t) = p_0 \delta(t) \tag{6}$$

where $\delta(t)$ is the Dirac delta function. The solution to the resulting initial boundary value problem applicable to the semi-infinite domain $x \in (0, \infty)$ is given by

$$\frac{p(t)}{p_0} = \exp(\Omega^2 t) \operatorname{Erfc}\left(\sqrt{\Omega^2 t}\right) \tag{7}$$

where $\operatorname{Erfc}(x)$ is the complementary error function defined by

$$\operatorname{Erfc}(x) = \frac{2}{\sqrt{\pi}} \int_x^\infty \exp(-\xi^2) d\xi \tag{8}$$

and

$$\Omega^2 = \left(\frac{A^2 K (nC_w + C_{\text{eff}})}{\eta V_w^2 C_w^2} \right) \tag{9}$$

The decay of the pressure pulse given by (7) contains known parameters except for the permeability K . The value of the permeability can be altered during the numerical evaluation of $p(t)$ so that the responses can be matched over the initial phases of the test when the conditions consistent with the semi-infinite domain are likely to be satisfied. Such a procedure can be used to estimate K .

Experimental procedure

This section outlines the details of the recovery of cores from block samples, the preparation of the cores for permeability testing, the experimental facilities used to conduct the tests and the results of typical tests.

Sample preparation

The cylindrical samples of the Lindsay Limestone used in the experimental research were obtained from a block sample of the rock supplied from the Saint Mary’s Quarry in Bowmanville, Ontario. The Lindsay Limestone outcrops



(a)



(b)

Fig. 3 Cores recovered from block samples of Lindsay Limestone from the Saint Mary’s Quarry, ON (core diameter, approximately 106 mm). **a** Samples recovered by coring perpendicular to the bedding planes, **b** samples recovered by coring along the bedding planes

at this location and the geological features of the limestone are consistent with what is documented for the limestone at depth. The cuboidal block samples of Lindsay Limestone measured approximately $0.45 \times 0.45 \times 1$ m and since the samples were recovered from a quarry, they displayed evidence of very sparse fracturing. It was, however, possible to recover samples of the rock, for the purposes of the experimental research that had no observable defects. The block samples were wet cored using diamond tipped corers. The dimensions of the cored samples varied depending on their proximity to fractures and the intact samples measured approximately 108-mm diameter and 100–300 mm in length. Cores were recovered both perpendicular to and along the bedding directions. Typical views of the recovered cores are shown in Fig. 3 and the colour contrast clearly illustrates the *nodular* nature of the Lindsay Limestone. The cored diameter was 108 mm and the core length was kept to a maximum to give sufficient length for machining purposes. The ends of the sample were cut perpendicular to the axis. The sample ends were machined parallel to form a 200-mm long sample, and the cylindrical

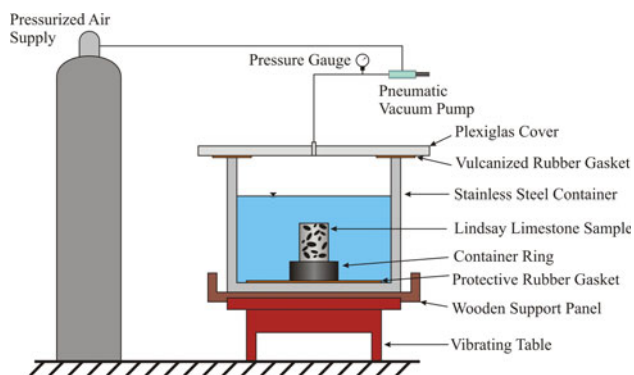


Fig. 4 A schematic layout of the experimental procedure for the saturation of the Lindsay Limestone samples

surface was machined to a precise diameter of 100 mm. These precise dimensions and smooth surface characteristics were necessary for companion tests that would be conducted under high confining pressures. During preparation of the sample, and particularly during machining, the sample was taped to prevent contamination.

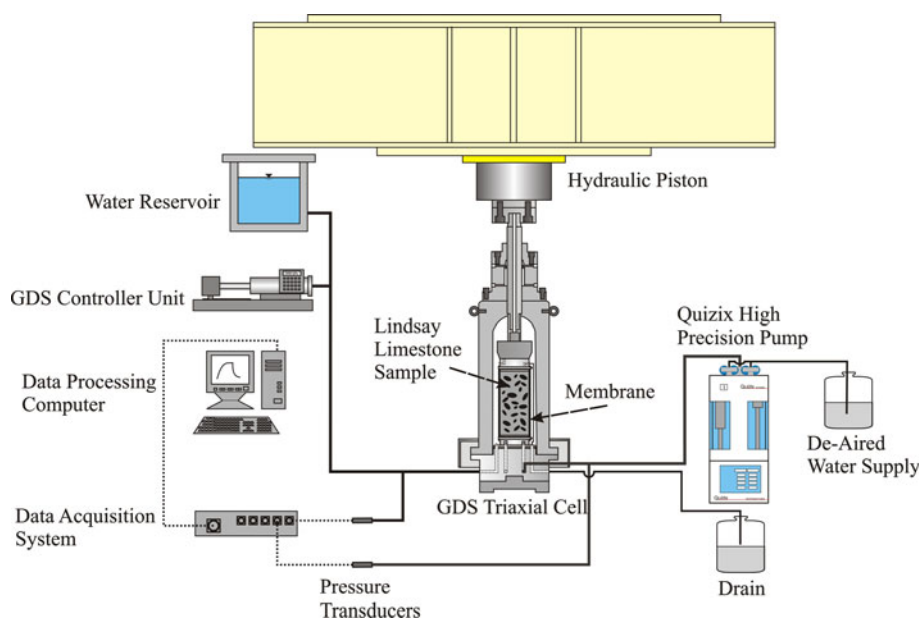
As was observed by Selvadurai (2009), the degree of saturation of the rock prior to hydraulic pulse testing can have a significant influence on the transient pulse decay. For this reason, the sample was saturated using a de-airing technique, which involved the application of a prolonged vacuum to a sample of the Lindsay Limestone, vacuuming and vibrating simultaneously during immersion in a 1- μm filtered water bath. Ideally, the pore fluid used in hydraulic pulse testing should be identical to that found at the location where the sample was retrieved. At large depths in the vicinity of the proposed DGR, the groundwater is saline and any tests performed on samples recovered from deep

boreholes should reflect the geochemical properties of the in situ ground water. In the current research investigations, however, the block samples were recovered from a shallow depth and at these locations the Lindsay Limestone can be exposed to the atmosphere and water influx for several decades. In this case, the use of distilled water to conduct the hydraulic pulse tests is justified. The details of the arrangement used to saturate the samples are shown in Fig. 4. Vacuum saturation was performed for 3 days and during this period expulsion of air from the sample was noted. After completion of the vacuuming sequence, the sample was allowed to remain in the water at a nominal pressure for a further 3 days to ensure that there was sufficient time for dissipation of any negative pressures that will develop during the saturation sequence. The exact time needed to either saturate or de-saturate the sample depends on the permeability of the Lindsay Limestone. The absence of air expulsion is regarded as a state of saturation and the same amount of time is allowed for the dissipation of excess pressures.

The experimental facility

The transient pressure pulse tests were conducted in a GDS high pressure triaxial chamber that could accommodate rock samples of diameter 100 mm and lengths up to 200 mm, dependent on the incorporation of an in-chamber load cell that can be used to measure deviatoric loads applied to the sample. The triaxial cell was chosen because of the ability to apply isotropic stress states to the sample consistent with the depth of sample recovery; the triaxial cell was also used quite successfully to examine the evolution of permeability hysteresis of Indiana Limestone

Fig. 5 The GDS Triaxial Cell and ancillary components of the test facility for conducting hydraulic pulse tests



subjected to isotropic compression (Selvadurai and Glowacki, 2008). Other components of the test facility included a Quizix precision pump (Model QX-6000-HC) to supply fluid flow to the sample at flow rates in the range 0.00034–50.00 ml/min with an accuracy of 0.1% of the set value. The pressure pulses were measured using a Honeywell Model TJE-200 g pressure transducer (Model 060-0708-12TJG; 0–200 psi gauge pressure, with an accuracy of 0.1% of full scale range) and all data acquisition was performed using components supplied by Measurements Computing. The acquisition of data was integrated using the Tracer DAQ Pro-software that allowed scanning rates up to 50 kHz. Although the pulse is applied over a finite time, the result relevant to the estimation of the permeability using the pulse test is the magnitude of the maximum initial pressure pulse and its decay with time. A schematic view of the experimental layout is shown in Fig. 5.

Sample assembly

The sample should be assembled in the GDS cell so that there is no possibility of leakage from the pressurizing chamber into the sample. The cell pressure is applied through a nitrile membrane supplied by Premier Industrial Hose Manufacturing Ltd. The unstretched internal diameter of the membrane was approximately 100 mm, with a wall thickness of approximately 3.2 mm. The sample is placed on the base pedestal and sealing is normally provided by stainless steel hose clamps that are located at the base and at the top of the sample. The seal between the nitrile membrane and the base pedestal and top cap is crucial to the reliable experimentation. It was observed that at pressures ranging from 5 to 20 MPa, a sealing agent was needed to develop the reliable seal. The base pedestal and the top cap and nitrile membrane were first cleaned using Sika Remover-208 and treated with Sika-Aktivator. The flexible sealant Sikaflex-221 was applied to all metal–nitrile membrane contacting surfaces, ensuring that a thin, but continuous coating was developed to provide the seal. The first hose clamp was then tightened around the base pedestal. The membrane was then filled with de-aired water and the lower porous steel diffuser disc was placed on the surface of the base pedestal. A prepared Lindsay Limestone core subjected to the saturation sequence described previously was then inserted into the nitrile membrane causing the water to force out any air trapped in the tubes leading to the sample and preventing drying of the sample. The upper porous metal diffuser is then inserted and the top cap and top of the membrane are cleaned and treated with Sika Remover-208 and Sika-Aktivator. The second hose clamp is placed over the membrane, and the Sikaflex-221 is applied to the top cap and to the top of the membrane. The

top cap is then inserted and the hose clamp fastened. The assembled sample is kept unpressurized for 24 h to allow drying of the sealants. Water is then pumped through the system in the absence of sealing pressure to remove any air that could have been trapped at the sample–nitrile membrane interface and within the pore space of the stainless steel diffuser discs. This sample assembly procedure was found to be highly effective and was followed during the assembly of both samples that were tested. The chamber of the GDS cell was filled with water and the confining pressure increased to its starting value of 5 MPa.

Experimental procedure and results

The outlet for fluid flow from the sample consisted of high pressure-resistant stainless steel, which allows unobstructed fluid efflux from the sample in a high pressure environment. The outer cell of the GDS triaxial cell was secured using a self-sealing arrangement and the maximum cell pressure that could be applied to the cell was 65 MPa. The pressurizing fluid can also be silicone oil, but this was not necessary for the range of pressures encountered in the current series of experiments. Once the triaxial cell was assembled, de-aired water was pumped through the sample to remove any further air that may have been released subsequent to the sample assembly procedure described in the previous section. This required the pumping of approximately 300 ml of water to fill the cell using a gravity feed. A critical criterion for conducting a reliable permeability test, either steady state or transient, is the establishment of a perfect seal between the sample and the sealing membrane. This was achieved by applying a cell pressure of 5 MPa; previous experiments (Selvadurai and Glowacki 2008), indicated that at this cell pressure level a perfect seal can be achieved between the membrane and an aluminum cylinder with a smooth surface. This starting level of cell pressure was maintained in all the hydraulic pulse tests conducted on the Lindsay Limestone. During application of this cell pressure, the inlet and outlet ports to the sample were allowed to drain to eliminate pressure build-up that could damage the sensors. The hydraulic pulse test was conducted by pumping de-aired water to the sample until a target pressure of 1 MPa was reached. Owing to the initial confining pressure of 5 MPa, the pressure pulse will not alter the contact between the sample and the pedestal. The duration for the attainment of the pressure was approximately 60 s, and the inlet valve was closed to shut-in the pressure. The valves used for this purpose were precision Swagelok Ball Valves that have no air entrapment during closure. The decay of the pressure pulse was continuously monitored for durations up to 5,000 s.

It is noted that the integrity of the sealing system is crucial to the success and validity of the experimental

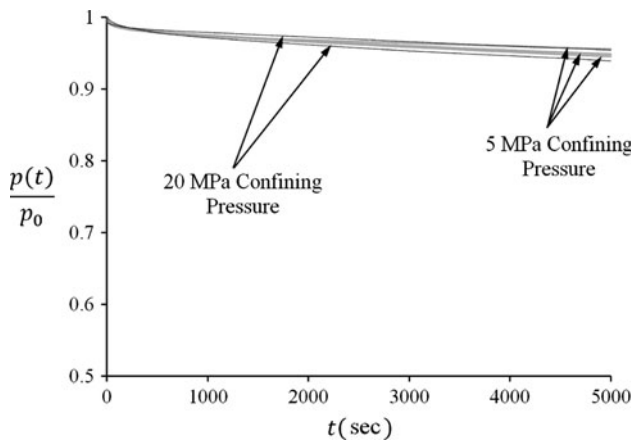


Fig. 6 Leakage curves conducted on a solid aluminum cylinder with identical experimental arrangements

procedures. Any leakage from the connections, valves, the sealing between the sample and the nitrile membrane and diffusion of water molecules into the nitrile membrane could, in principle, influence the results of the experiments. The issue of possible leakage through the membrane can be excluded from the discussion, since such a leak would have been recorded as a drastic increase in the upstream pressurization boundary and rapid water efflux from the downstream boundary. The fluid pressure in the pressurizing chamber also remained unchanged during these additional tests. The question of leakage through the components, including valves and connections was examined by conducting a pulse test where the sample was a solid aluminum cylinder of diameter 100 mm and length 200 mm. The experiment was performed at both 5 and 20 MPa of confining pressure. The duration of the test was approximately 5,000 s and Fig. 6 illustrates the typical decay curves that have been observed for the system leakage for tests conducted at both 5 and 20 MPa. It is clear that the increase in cell pressure does not result in any change in the decay rate. This suggests that the seal between the sample and the membrane is sound and the system leakage is most likely due to factors associated with the components of the pressurizing system. The permeability corresponding to the leakage can be quantified in terms of an “apparent permeability” and this is estimated at approximately $3 \times 10^{-23} \text{ m}^2$ (which is an order of magnitude lower than the estimated permeability of the Lindsay Limestone).

Analysis of experimental results

To estimate the permeability of the tested Lindsay Limestone using the experimental data, additional mechanical and physical parameters are needed. The mechanical

parameter relates to the compressibility of the porous skeleton; this is estimated by determining the Young’s modulus and Poisson’s ratio for the unsaturated porous skeleton: i.e.

$$C_{\text{eff}} = \frac{3(1 - 2\nu_{\text{eff}})}{E_{\text{eff}}} \quad (10)$$

The Young’s modulus and Poisson’s ratio were determined by conducting uniaxial compression tests on instrumented samples of the Lindsay Limestone. Several samples were first tested to failure to determine the compressive strength of the limestone. The elasticity parameters were determined by subjecting the instrumented samples to stress levels approximately one-third the peak stress and by repeating the tests over several cycles of quasi-static loading and unloading. Poisson’s ratio for the Lindsay Limestone was determined from the record of the lateral strains during axial compressions. The average Young’s modulus for the Lindsay Limestone obtained from these experiments was approximately 21 GPa and Poisson’s ratio was approximately 0.25. Corresponding values available in the literature (Golder Associates 2003) are 35 GPa and 0.30, respectively. The porosity of the Lindsay Limestone was estimated from saturation drying tests conducted on several sizes of samples. The visual observations of inhomogeneities in the samples point to possible multiple levels of porosity, although in the present investigations, the porosity is specified within the range 0.01–0.04. The published literature (Gartner Lee Ltd 2008) cites a value of 0.02 for the porosity. Mercury Intrusion Porosimetry (MIP) tests were also conducted at the AECL Laboratories in Pinawa, Man. In these tests, the porosity varied between 0.0675 and 0.135 and well outside the range of porosity observed in other investigations. The effectiveness of MIP tests for rocks of very low permeability thus needs to be re-assessed. Processes, such as micro-fracturing during mercury injection could lead to abnormally high estimates of the porosity. The remaining parameter needed to perform the computations for an assigned value of K is the volume of the fluid mass that experiences expansion during the pressure decay. It is assumed that the porous steel disks, the valves, the diaphragm of the pressure transducer, the connecting tubes and any part of the nitrile membrane in contact with the pressurized region experience negligible volume change at the pressures applied to create the hydraulic pulse. The volume of water in the pressurized region was determined by weighing all the valves and fixtures in a fully saturated condition and subtracting the weight in an air-dried condition. The volume of water in the porous stainless steel disk at the inlet end of the sample was determined in a similar manner. The estimated values of the parameters required to develop the decay curves are as follows:

Compressibility of the porous skeleton (C_{eff}) = (7.22) 10^{-8} m^2/kN

Compressibility of the pore water at 21°C (White 1986) (C_w) = (454.1) 10^{-9} m^2/kN

Dynamic viscosity of water at 21°C (η) = 10^{-6} $kN s/m^2$

Nominal porosity of the limestone (n) = 0.015

Area of cross section of the limestone sample (A) = 0.007854 m^2

Volume of water in the compressed region (V_w) = (29.9) 10^{-6} m^3 (thick end plate)

Volume of water in the compressed region (V_w) = (18.75) 10^{-6} m^3 (thin end plate)

These values give

$$\Omega^2 = \left(\frac{A^2 K (nC_w + C_{eff})}{\eta V_w^2 C_w^2} \right) = \begin{cases} (67.252) K s^{-1} & \text{for thin porous plates} \\ (26.402) K s^{-1} & \text{for thick porous plates} \end{cases} \quad (11)$$

where K is expressed in m^2 . There are several procedures that can be used to estimate the permeability of the tested rock using experimental data and the theoretical relationships. The method used here follows the procedures proposed by Selvadurai and Carnaffan (1997) and Selvadurai et al. (2005), which involves assigning a range of values of K in the expressions (7) and (11), so that a set of experimentally determined pulse decay curves can be completely bounded. This procedure will result in a set of bounds for the permeability of the Lindsay Limestone rather than a specific value. The theoretical estimates for the decay curves applicable to both values of porosity are included for purposes of reference. The justification for the procedure is self-evident since all the material and physical parameters (C_{eff} , C_w , η , n , V_w and A) used to generate the theoretical pulse decay curves will themselves have error estimates; a more rigorous approach will involve a complete error analysis of the result (7), which perhaps is not altogether justified. The corrected pressure pulse decay curves for tests conducted on two samples of the Lindsay Limestone cored perpendicular to the nominally identifiable bedding plane, at the reference confining pressure of 5 MPa are shown in Fig. 7. For the Sample 1, the permeability can be assigned the range $K \in (0.2, 0.5) 10^{-22}$ m^2 and for the second sample, the permeability range corresponds to $K \in (1.1, 2.7) 10^{-22}$ m^2 . There are no observable reasons for the apparent variations in the measured permeability. When considering the composite of results, the permeability for the samples tested with flow induced perpendicular to the bedding plane and at the confining pressure of 5 MPa can be assigned the range $K \in (0.2, 2.7) 10^{-22}$ m^2 . The values reported in the literature (Golder Associates 2003) are in the range

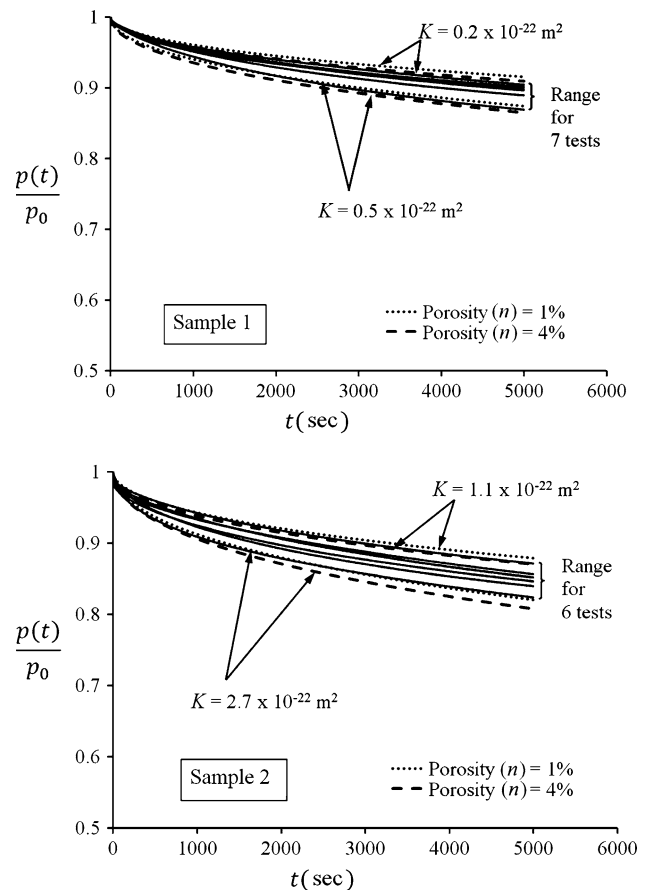


Fig. 7 The results of hydraulic pulse tests conducted on two samples of the Lindsay Limestone (reference confining pressure of 5 MPa)

$K \in (2.00 \text{ to } 21.00) 10^{-22}$ m^2 . The fact that the permeability estimates determined from this research investigation are lower than those reported in the literature indicates that the experimental technique is reliable in terms of little or no leakage from the facility, from the connections, from the interface between the membrane and the rock specimen or existence of fractures in the specimen, which would have certainly contributed to a much higher estimate for the bulk permeability of the rock sample. The corresponding results for the corrected pressure pulse decay curves for tests conducted on a sample cored perpendicular to the bedding plane and at the reference confining pressure of 20 MPa are shown in Fig. 8. For the Sample 1, the permeability can be assigned the range $K \in (1.2, 2.5) 10^{-22}$ m^2 and for the second sample, the permeability range corresponds to $K \in (4.2, 7.5) 10^{-22}$ m^2 . For the first two samples, there is consistency in the measured values in the sense that the Sample 1 gave results that were lower than the Sample 2. The results of the estimates indicate that at the reference confining pressure of 20 MPa, the permeability of the tested samples of the Lindsay Limestone can be assigned the range.

As a supplement to this series of tests, permeability tests were also conducted on the samples of the Lindsay

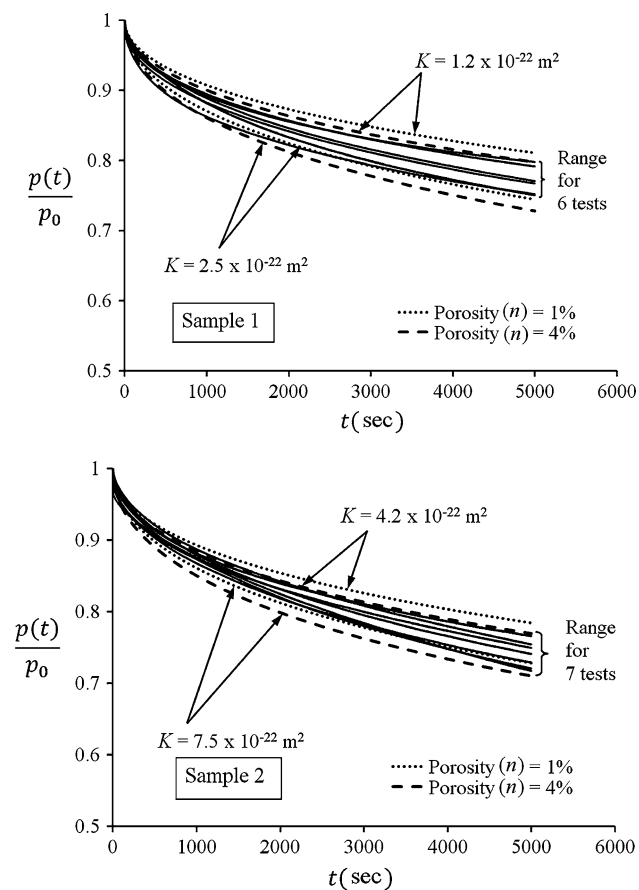


Fig. 8 The results of hydraulic pulse tests conducted on two samples of the Lindsay Limestone (reference confining pressure of 20 MPa)

Limestone cored perpendicular to the bedding plane, at stages of 5 MPa, increasing up to a cell pressure of 20 MPa. In this series of tests, the cell pressure was increased in stages and the pore fluid pressure in the sample was allowed to remain unaltered during the application of the cell pressure. This provides some degree of assurance that the surface region of the cylindrical sample where the pulse tests are performed is not subjected to excess fluid pressures. Between 3 and 9 hydraulic pulse tests were conducted on each sample and at each stress level and the fluid pressure applied to conduct the pulse test was maintained at 1 MPa. The evolution of permeability in the samples of Lindsay Limestone with increasing confining pressure up to 20 MPa and its subsequent reduction to the reference confining pressure of 5 MPa are shown in Fig. 9. For ease of comparison, the results for the cell pressure-induced alteration in the permeability in the samples are presented as absolute values so that the influence of the isotropic stress history can be easily observed.

During the increase in the cell pressure up to 20 MPa, both samples displayed an increase in the permeability (increases of approximately 5.8 times for the sample 1 and 3.1 for the sample 2 (these are estimated using the averages

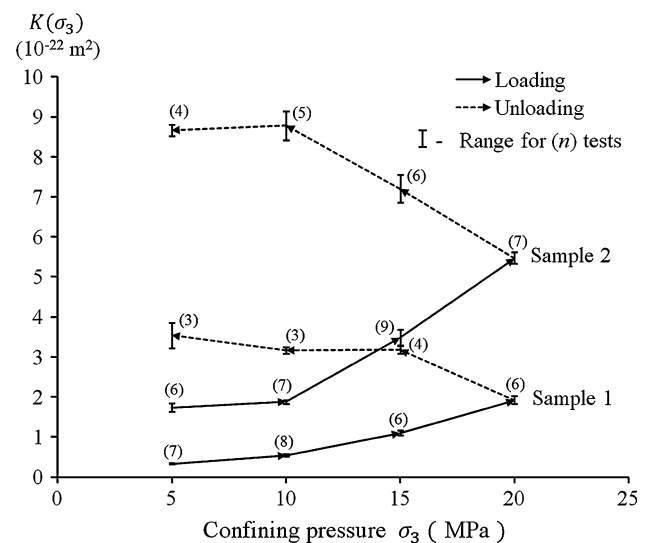


Fig. 9 Variation of permeability of the Lindsay Limestone during a quasi-static load cycle (results derived from 81 pulse tests conducted on two samples)

of individual curve fits). The permeability of the samples was also measured during the unloading of the cell pressure from 20 to 5 MPa, again in stages of 5 MPa. At the end of the quasi-static cell pressure cycle, both samples experienced increases in the permeability; increases of approximately 10.7 for sample 1 and approximately 5.0 for sample 2 (again, these are estimated using the averages of individual curve fits). This is in contrast to the irreversible order of magnitude decrease in permeability with increase in confining stress that was observed in the experimental investigations reported by Selvadurai and Głowacki (2008), albeit for Indiana Limestone, which has a relatively uniform structure. In addition, the studies by Vilks and Miller (2007) indicate that the permeability of the Lindsay Limestone at Cobourg, perpendicular to the bedding plane was approximately $(3.5) \cdot 10^{-22} \text{ m}^2$ at a confining pressure of 4.7 MPa and approximately $(2.0) \cdot 10^{-22} \text{ m}^2$ at a confining pressure of 9.5 MPa. These tests, however, were carried out on samples with a core length of 1.5 cm. and a surface area of 4.91 cm^2 . It should be noted that the nodular inclusion-type features can be approximately 2 cm in dimension. At this scale, sample preparation itself can induce damage that can influence test results of permeability. Permeability decrease with an increase in isotropic compression is perhaps the norm for structurally relatively uniform rocks such as sandstones, limestones and granite (David et al. 1994; Wong et al. 1997; Suri et al. 1997; Zhu and Wong 1997; Heidland 2003; Selvadurai 2004) and such effects could be attributed to pore closure, pore collapse, and the closure of defects at the inter-granular and intra-granular levels. Further references to in situ permeability evaluations also point to a decrease in the

permeability with depth, resulting from an increase in the net isotropic stress state with depth (see e.g. Banks et al. 1996). Finally, the possibility of both hydraulic and elastic transverse isotropy due to the nominal presence of a stratified structure in this material requires further investigation. The elastic transverse isotropy can influence the effective skeletal compressibility of the rock that can influence the interpretation of the results.

Conclusions

The argillaceous Lindsay Limestone has a nodular fabric where the inhomogeneities point to distinct arrangements either perpendicular to the bedding plane or along the bedding plane and such features could in general result in a possible directional dependence in both the mechanical and fluid transport characteristics. This phase of the research program focused on the estimation of the permeability characteristics of the rock perpendicular to the bedding plane, using results of axial flow hydraulic pulse tests. The estimates for the permeability obtained from this research are lower than values available from investigations conducted in connection with the assessment of hydraulic properties at depths corresponding to a proposed Deep Geologic Repository. The experimental investigations were extended to include an evaluation of the permeability of the Lindsay Limestone during the application of an isotropic confining pressure. The results of these tests point to the potential increase in the permeability of the rock with increasing isotropic stress. This is in stark contrast to the usual observation of an irreversible decrease in the permeability of relatively uniform rocks due to effects such as pore closure and pore collapse mechanisms. This reverse trend seems to suggest that the noticeable inhomogeneity in the sample can be a source of micromechanical damage or cracking at inter-nodular boundaries that could result in the observed increase in the permeability. It also suggests the possibility of the development of complex three-dimensional stress states in the internal fabric of the rock even during the application of isotropic external stress fields and these can contribute to increasing permeability evolution. The experiments further point to a continued increase in the permeability of the rock during the unloading of the isotropic confining pressure. These results are an anomaly, where the normal manifestation to a reduction in the applied cell pressure is the closure of micro-fissures that would lead to some measure of recovery or reduction of the permeability. The results nonetheless point to the need for further experimental investigations to establish the process of permeability evolution in rocks with a dominant internal fabric under applications of generalized states of stress.

Acknowledgments The work described in this paper was supported by a Strategic Research Grant awarded by the Natural Sciences and Engineering Research Council of Canada to the senior author. The authors are grateful to Mr. Mark Jensen and Dr. Ben Belfadhel of the Nuclear Waste Management Organization, Toronto, ON, for their interest in the research and to Dr. S. Stroes-Gascoyne for allowing access to results of MIP tests conducted at the AECL Laboratories, Pinawa, Man. The technical assistance of Mr. J. Bartczak, of the Environmental Geomechanics Laboratory at McGill University in developing the uses of the Sika sealant technique is acknowledged. The assistance of Mr. Nick Papanicolaou, Quarry Coordinator, St. Mary's Cement, Bowmanville, ON, for providing the research program with the block samples of the Lindsay Limestone is also gratefully acknowledged.

References

- Alonso E, Gens A, (eds) (2002) Key issues in waste isolation research. *Eng Geol* 64:89–316
- Alonso EE et al (2005) The FEBEX benchmark test: case definition and comparison of modelling approaches. *Int J Rock Mech Min Sci* 42:611–638
- Armand G, Su K (2006) Hydromechanical coupling phenomena observed during a shaft sinking experiment in a deep argillaceous rock. *Proc GeoProc* 2006, Nanjing, pp 725–731
- Banks D, Odling NE, Skarphagen H, Rohr-Torp E (1996) Permeability and stress in crystalline rock. *Terra Nova* 8:223–235
- Barenblatt GI, Entov VM, Ryzhik VM (1990) Theory of fluid flows through natural rocks. Kluwer, Dordrecht
- Bear J (1972) Dynamics of fluids in porous media. American Elsevier, New York
- Bernabé Y (1986) The effective pressure law for permeability in Chelmsford Granite and Barre Granite. *Int J Rock Mech Min Sci* 23:267–275
- Bernabé Y (1987) A wide range permeameter for use in rock physics. *Int J Rock Mech Min Sci* 24:309–315
- Brace WF, Walsh JB, Frangos WT (1968) Permeability of granite under high pressure. *J Geophys Res* 73:2225–2236
- Chapman NA, McKinley IG (1987) The geological disposal of nuclear waste. Wiley, New York
- David C, Wong T-F, Zhu W, Zhang J (1994) Laboratory measurement of compaction-induced permeability change in porous rocks: Implications for the generation and maintenance of pore pressure excess in the crust. *Pure Appl Geophys* 143:425–456
- Gartner Lee Ltd (2008) DGR supporting technical report: phase I geosynthesis. OPG 00216-REP-01300-00010-R00 (DOC 556)
- Gnirk P (1993) OECD/NEA International Stripa Project Overview—Natural Barriers. SKB, Stockholm
- Golder Associates (2003) Low level waste geotechnical feasibility study—Western Waste Management Facility Bruce Site, Tiverton, Ontario. Report to Ontario Power Generation
- Gray MN (1993) OECD/NEA International Stripa Project Overview, vol III: Engineered Barriers. SKB, Stockholm
- Gross J, Scherer GW (2003) Dynamic pressurization: novel method for measuring fluid permeability. *J Non-Crystalline Solids* 325:34–47
- Heidland J (2003) Laboratory testing of coupled hydro-mechanical processes during rock deformation. *Hydrogeol J* 11:122–141
- Horseman ST (2001) Self-healing of fractures in argillaceous media from the geomechanical point of view. In: Self-healing topical session. Proceedings of 11th Clay Club Meeting, Nancy. OECD/NEA, Paris, pp 19–25
- Hoteit N, Su K, Tijani M, Shao J-F (eds) (2002) Hydromechanical and thermohydromechanical behaviour of deep argillaceous

- rock-theory and experiments. Proceedings of international workshop on geomechanics. Paris A.A. Balkema Publications Lisse, The Netherlands
- Hsieh PA, Tracy JV, Neuzil CE, Bredehoeft JD, Silliman SE (1981) A transient method for determining the hydraulic properties of 'tight' rocks.—I. Theory. *Int J Rock Mech Min Sci* 18:245–252
- Hueckel T, Peano A (eds) (1996) Thermo-mechanics of clays and clay barriers. *Spec Issue Eng Geol* 41:1–301
- Huertas F et al (2000) Full-scale engineered barriers experiment for a deep geological repository for high-level radioactive waste in crystalline host rock. European commission nuclear sciences and technology, EUR 19147, Brussels
- Intera Ltd (1988) Inventory and assessment of hydrogeologic conditions of underground openings in sedimentary rock. Representative of Ontario Hydro
- Laughton AS, Roberts LEJ, Wilkinson D, Gray DA (1986) The disposal of long-lived and highly radioactive wastes. In: Proceedings of a Royal Society Discussion Meeting London, Royal Society, London
- Maßmann J, Uehara A, Rejeb A, Millard A (2009) Investigation of desaturation in an old tunnel and new galleries at an argillaceous site. *Environ Geol* 57:1337–1345
- Mazurek M (2004) Long-term used nuclear fuel waste management—geoscientific review of the sedimentary sequence in Southern Ontario. Technical Report TR 04-01, Institute of Geological Sciences, University of Bern, Switzerland
- Millard A, Rejeb A (2008) Investigation of the hydro-mechanical in situ properties of Tournemire Argillite from the mine-by-test experiment. In: Shao J-F, Burlion N (eds) Thermo-hydromechanical and chemical coupling in geomaterials and applications. Proceedings of the third international symposium Geoproc' 2008. Lille, France, pp 313–320
- Neuzil CE, Cooley C, Silliman SE, Bredehoeft JD, Hsieh PA (1981) A transient method for determining the hydraulic properties of 'tight' rocks—II Application. *Int J Rock Mech Min Sci* 18:253–258
- OECD (1988) Geological disposal of radioactive waste. In situ research and investigations in OECD countries. NEA OECD, Paris
- OPG (2008) Ontario power generation's deep geologic repository for low and intermediate level waste. Supporting technical report: phase 1-geosynthesis. OPG 00216-REP-01300-00010-R00
- Philips OM (1991) Flow and reactions in permeable rocks. Cambridge University Press, Cambridge
- Pusch R (ed) (1990) Artificial clay barriers for high-level radioactive waste repositories. *Spec Issue Eng Geol* 28:230–455
- Raven K, Novakowski KS, Yager RM, Heystee RJ (1992) Supernormal fluid pressures in sedimentary rocks of southern Ontario—Western New York State. *Can Geotech J* 29:80–93
- Selvadurai APS (ed) (1997) Hydro-thermo-mechanics of engineered clay barriers and geological barriers. *Spec Issue Eng Geol* 47:311–379
- Selvadurai APS (2000) Partial differential equations in mechanics, vol 1. Fundamentals Laplace's equation diffusion equation wave equation. Springer, Berlin
- Selvadurai APS (2002a) Influence of pressurized water influx on the hydro-thermal behaviour of an engineered clay barrier in a waste emplacement bore hole. *Eng Geol* 64:157–178
- Selvadurai APS (2002b) Some remarks on the elastic drive equation. In: Environmental geomechanics. In: Vulliet L, Laloui L, Schrefler BA (eds) Proceedings of the international workshop on environmental geomechanics, Monte Verita, Ascona. EPFL Press, Lausanne, pp 253–258
- Selvadurai APS (2004) Stationary damage modelling of poroelastic contact. *Int J Solids Struct* 41:2043–2064
- Selvadurai APS (2009) Influence of residual hydraulic gradients on decay curves for one-dimensional hydraulic pulse tests. *Geophys J Int* 177:1357–1365
- Selvadurai APS, Carnaffan P (1997) A transient pressure pulse method for the measurement of permeability of a cement grout. *Can J Civil Eng* 24:489–502
- Selvadurai APS, Głowacki A (2008) Permeability hysteresis of limestone during isotropic compression. *Ground Water* 46:113–119
- Selvadurai APS, Nguyen TS (1996) Scoping analyses of the coupled thermal-hydrological-mechanical behaviour of the rock mass around a nuclear fuel waste repository. *Eng Geol* 47:379–400
- Selvadurai PA, Selvadurai APS (2007) On cavity flow permeability testing of a sandstone. *Ground Water* 45:93–97
- Selvadurai APS, Selvadurai PA (2010) Surface permeability tests: experiments and modelling for estimating effective permeability. *Proc R Soc Math Phys Sci Ser A* 466:2819–2846
- Selvadurai APS, Boulon MJ, Nguyen TS (2005) The permeability of an intact granite. *Pure Appl Geophys* 162:373–407
- Song I, Renner J (2006) Linear pressurization method for determining hydraulic permeability and specific storage of a rock sample. *Geophys J Int* 164:685–696
- Suri P, Azeemuddin M, Zaman MM, Kukreti AR, Roegiers J-C (1997) Stress-dependent permeability measurement using the oscillating pulse technique. *J Pet Sci Eng* 17:247–264
- Vilks P, Miller NH (2007) Evaluation of experimental protocols for characterizing diffusion in sedimentary rocks, atomic energy of Canada limited. Nuclear Waste Management Division Report TR-2007-11, Toronto
- White FM (1986) Fluid mechanics, 2nd edn. McGraw-Hill, New York
- Wong T, David C, Zhu W (1997) The transition from brittle faulting to cataclastic flow in porous sandstones: mechanical deformation. *J Geophys Res* 102:3009–3025
- Zhu W, Wong T (1997) The transition from brittle faulting to cataclastic flow: permeability evolution. *J Geophys Res* 102:3027–3041